A neutron scattering study of the amorphization reaction in a $Ni_{50}Mo_{50}$ alloy

1993 J. Phys.: Condens. Matter 5 5235

(http://iopscience.iop.org/0953-8984/5/30/003)

J. Phys.: Condens. Matter 5 (1993) 5235–5244. Printed in the UK

A neutron scattering study of the amorphization reaction in a $Ni_{50}Mo_{50}$ alloy

Li Meiya†, S Enzo‡, I Soletta§, N Cowlam† and G Cocco§

† Department of Physics, University of Sheffield, Sheffield S3 7RH, UK

‡ Dipartimento di Chimica Fisica, Università di Venezia, Calle Larga S Marta 2137, 30123 Venezia, Italy

§ Dipartmento di Chimica, Università di Sassari, via Vienna 2, 07100 Sassari, Italy

Received 16 December 1992

Abstract. The solid state amorphization reaction in $Ni_{50}Mo_{50}$ alloys has been investigated by neutron diffraction and neutron small-angle scattering. A series of specimens has been mechanically alloyed for 2, 4, 8, 16 and 32 hours in a high-energy ball mill. The initial stages of the reaction are characterized by the deformation of the parent crystalline phases. After 8 hours of treatment a change in the samples is observed and those treated for 16 and 32 hours consist of an amorphous NiMo phase with some free molybdenum. The intensity of the small-angle scattering is much greater for the 2 hour specimen than for the parent, but decreases regularly for longer milling times. The Guinier plots show considerable curvature indicative of particles with a range of sizes. Graphs of log $I(Q)$ versus log Q show a sequence of changes which correspond to the sequence of changes seen in the diffraction data. The graphs for the 2 and 4 hour samples are linear over an extended range of scattering vector Q. The slope of these graphs is about -3.4, which is indicative of a rough surface having the fractal dimension of 2.6. We tentatively associate this with the convoluted surfaces between the nickel and molybdenum particles which are drawn into an interpenetrating filamentary structure in the early stages of the mechanical alloying process.

1. Introduction

There has been considerable interest recently in amorphous metallic alloys produced by solid state reactions, particularly by the mechanical alloying (MA) of crystalline metal powders [1,2]. One of the basic problems associated with this method of synthesis is establishing whether the end product has a genuine amorphous structure on an atomic scale or whether it is micro-crystalline or nano-crystalline. It seems likely that all three types of structure can occur. In addition, it is probably necessary to consider every new system on an individual basis. This is quite unlike the case of metallic alloy glasses where, after some initial uncertainty [3], almost all examples were regarded without question as being truly amorphous.

We have recently verified by neutron and x-ray diffraction studies, that truly amorphous CuTi alloys may be obtained in the concentration range $50\% \leqslant Cu \leqslant 75\%$ after 16 hours of MA treatment [4]. Furthermore, the amorphization reaction in the CuTi system can extend over a wider composition range in specimens having gaseous contaminants [5]. We judged it appropriate, now being aware of the significance of gaseous contamination in the samples by these neutron studies, to concentrate on the atomic scale changes by which the amorphization reaction proceeds. We have chosen for this samples where there is less possibility of gaseous contamination so that we may investigate the reduction of crystallite size and the distribution of internal strain in the crystallites as the reaction proceeds [6]. These factors

0953-8984/93/305235+10$07.50

can be determined simultaneously from a diffraction pattern providing a proper analysis is made of the Bragg peak broadening as a function of scattering vector $Q = 4\pi \sin(\theta)/\lambda$ [7]. However the values of average particle size and of lattice strain content as a function of MA time which have been reported in the literature are not in very good agreement [8–10]. This is not just because of the different systems studied by these authors, but also because of the different methods of analysis used. The application of the simple Scherrer [6] equation to a very wide Bragg peak, for example, may give an underestimate of the particle size, because the broadening may also be due to the effects of structural disorder and relaxation when the crystallite size is small. This shortcoming of the analysis may be avoided by using multiple-peak methods, such as those developed by Warren and Averbach [11] and by Williamson and Hall [12]. Even so, the extrapolation procedure to $Q = 0$ of peak shape (WA) or width (WH), where the strain broadening is supposed absent, may still bias the average crystallite size obtained. The application of these methods of analysis can be made most successfully with a diffraction pattern having several peaks of satisfactory intensity at high Q values. This is difficult to achieve with x-rays because of several inherent limitations. Firstly the wavelength of the commonly used Cu Kα radiation sets a practical limit on the scattering vector of $Q = 8$ Å^{-1}, while the form factor dependence of the x-ray scattering causes a rapid decrease in the intensities of the Bragg peaks with increasing Q values. In addition, the overlap of adjacent peaks due to peak broadening can create a problem, which is sometimes exacerbated by the growth of intermediate products in the solid state reaction, such as intermetallic compounds [13]. Some of these problems can, in principle, be resolved with the aid of neutron diffraction. Firstly, the scattering is isotropic, so that the fall in intensity of the Bragg peaks with increasing Q value is reduced and depends only on the geometrical and temperature effects. Secondly, the use of pulsed neutron scattering with a white incident beam [14] offers the opportunity of recording diffraction patterns to Q values of 30–50 Å^{-1}. In addition, the related technique of neutron small-angle scattering (SAS) offers an independent method of determining the average particle sizes in powders produced by the MA method. Whilst care must be taken to allow for surface effects in all SAS measurements, the low absorption of neutrons for most materials means that it has advantages over x-ray SAS in examining the bulk of specimens. In the present paper we shall give a preliminary account of some neutron diffraction and neutron SAS measurements on $Ni_{50}Mo_{50}$ alloys prepared by the MA technique.

2. Sample preparation and experimental method

The samples were produced using nickel and molybdenum powders of 99.99% purity supplied by Alfa Products, which were mixed in the proportion 38 weight percent nickel and 62 weight percent molybdenum to make the equiatomic alloy $Ni_{50}Mo_{50}$. The powders were milled in a hardened steel vial using a Spex Mixer Mill (model 8000). The ball-to-powder ratio was 10:1 using balls of $\frac{1}{2}''$ diameter. The milling was carried out under an argon atmosphere to prevent oxidation. Five samples were produced in addition to the parent (0 hours), namely MA treated for 2, 4, 8, 16 and 32 hours. An x-ray examination of these samples was made through the first broad diffraction halo, immediately after the MA treatment, in order to confirm their structure. A scan of 30° to 60° in steps of 0.05° was made using a Siemens D500 diffractometer and copper Kα radiation $\lambda = 1.54178$ Å. The neutron diffraction experiments were made using the LAD instrument [15] at the ISIS neutron source, Rutherford Appleton Laboratory, Chilton. The specimens were measured in thin-walled vanadium tubes of 6 mm internal diameter which were weighed full of powder to permit a normalization to be made between the different specimens. Table 1 shows that

with the exception of the parent sample, for which the packing was presumably different, the sample weights were rather similar. A scan with an empty tube, a vanadium normalization and background determination were also made. The run times for samples of about 4 g varied between 3 hours for the crystalline samples and 11 hours for the amorphous samples. The neutron SAS measurements were made on the LOQ instrument [16], also at ISIS. The powders were placed in 'Helma' brand quartz cells of 1 mm beam path and were illuminated with a neutron beam 8 mm in diameter for run times of one hour duration. A measurement with an empty quartz cell and a vanadium normalization scan were also made together with transmission measurements of all the specimens.

Table 1. The specification of the six $Ni_{50}Mo_{50}$ samples given as function of MA time.

MA time	0	2	4	8	16	32
Weight	4.445	5.177	5.174	5.026	4.966	5.114
Normalized sum of Bragg peak intensities						
Nickel peaks	4.428	3.886	3.495	0.806	—	—
Molybdenum peaks	2.267	2.064	2.047	1.151	0.984	1.063
Fractions of the parent elements consumed						
Nickel	0.000	0.127	0.211	0.818	1.000	1.000
Molybdenum	0.000	0.090	0.097	0.500	0.566	0.531
Constitution of the composite samples (%)						
Nickel	50	44	40	9	0	0
Molybdenum	50	45	45	25	22	23
a–NiMo phase	0	11	15	66	78	77
Composition of a–NiMo phase	—	$Ni_{59}Mo_{41}$	$Ni_{68}Mo_{32}$	$Ni_{62}Mo_{38}$	$Ni_{64}Mo_{36}$	$Ni_{65}Mo_{35}$

3. Experimental results

Figure 1 shows a comparison between parts of the neutron and x-ray diffraction patterns in a Q range selected to show the molybdenum (110) and the nickel (111) and (200) Bragg peaks of the parent unmilled powders. It can be seen from the peak half-widths that the instrumental resolution is slightly better in the x-ray case and this is consistent with LAD being a dual purpose neutron instrument intended for work on amorphous and crystalline samples. The x-ray scattering is proportional *inter alia* to the square of the atomic number and so the intensity of scattering from a molybdenum atom is more intense than from a nickel atom, in the ratio $(46/28)^2$. For neutrons this is reversed and the nuclear scattering amplitude of nickel $b_{Ni} = 1.03 \times 10^{-12}$ cm is larger than that of molybdenum $b_{Mo} = 0.695 \times 10^{-12}$ cm and in fact, is one of the largest values in the periodic table. This means that the structural changes in the nickel during the MA process can be more easily followed with neutrons than with x-rays. The two techniques are therefore complementary to one another and the present study augments the x-ray and EXAFS investigations already made by us on these NiMo alloys [17, 18]. The neutron diffraction patterns of the $Ni_{50}Mo_{50}$ specimens were derived from the raw spectra by correcting for counter dead-time, normalizing to the spectrum of the incident beam monitor and converting from time-of-flight units to scattering vector Q [19]. The patterns obtained are given as a function of MA time in figure 2. They are given over a Q range of 2 $Å^{-1}$ to 21 $Å^{-1}$ and plotted as the logarithm of the neutron intensity in order to improve the visibility of the small peaks at high Q values. A significant

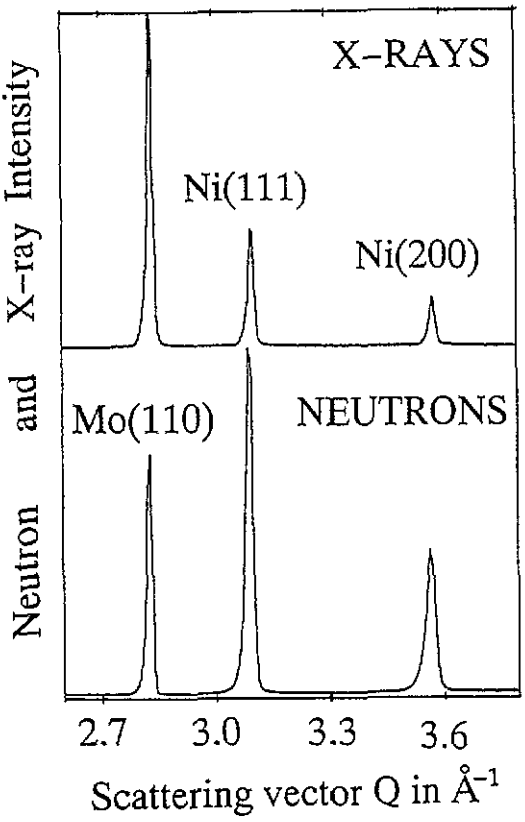

Figure 1. A comparison is given between the x-ray and neutron diffraction pattern in the Q range where Mo (110), Ni (111) and Ni (200) occur. The relative intensities of the Bragg peaks from the nickel and the molybdenum are reversed for the two radiations because of the different magnitudes of the scattering amplitudes.

feature of this figure is the lack of any sloping background due to neutron inelastic scattering from hydrogen [5]. This indicates that these samples are uncontaminated. Also all the peaks in the pattern of the parent sample (0 hours) can be identified as being from just the molybdenum BCC and the nickel FCC phases. The peak broadening in this pattern is due to instrumental effects alone and the small discontinuities which can be seen in the background, such as that at $\simeq 4$ Å^{-1} are artefacts of the (vanadium) normalization. It is easily seen from the figure that the envelope of the Bragg peaks decays progressively as the milling time increases. A preliminary analysis suggests that *relative* peak intensities remain sensibly constant [20], however we propose to develop methods of analysing the Bragg *peak envelope itself* more fully later. Figure 2 shows that the parent, 2 and 4 hour samples consist of progressively damaged crystalline phases of nickel and molybdenum. After 8 hours of MA treatment changes are observed in the diffraction pattern and the 16 and 32 hour samples consist of an amorphous NiMo alloy which gives a characteristic diffuse diffraction pattern with small Bragg peaks superimposed. This indicates that not all of the molybdenum has been consumed in the reaction. The changes seen in the different diffraction patterns of figure 2 as a function of MA time are in excellent agreement with those observed by us previously using x-ray diffraction [17, 18, 21]. The reduction of the time-of-flight SAS data from LOQ [22] is more complex than for the fixed wavelength case. The data from the area detector were converted to radial averages and when the background or container scattering was removed, the data were scaled to data from a sample of known cross-section. Figure 3 shows the SAS intensity $I(Q)$ for the six NiMo samples, over a Q range of 0.006 Å^{-1} to 0.025 Å^{-1}. A distinct signal is seen from the parent specimen, but that from the sample MA for 2 hours is almost three times as great. The signals for samples

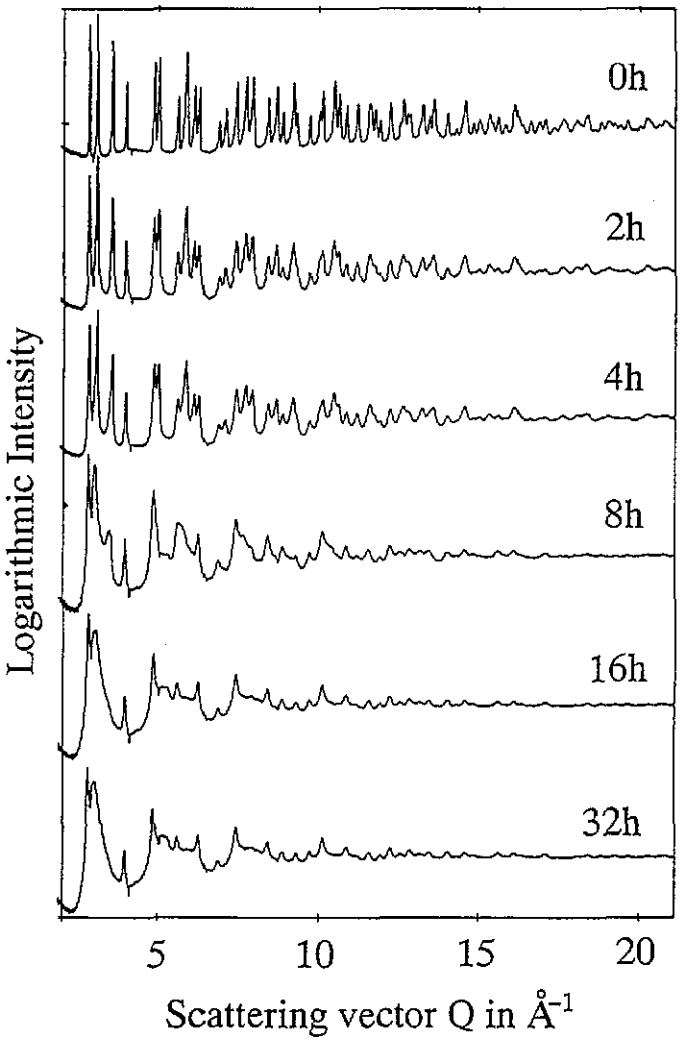

Figure 2. The neutron diffraction patterns of the six $Ni_{50}Mo_{50}$ samples are given, plotted as the log of intensity against the scattering vector Q. After 16 hours of MA treatment the Bragg peaks from the parent crystalline nickel are absent from the diffraction patterns.

milled for longer periods fall progressively so that for the 32 hour sample is just 20% of that of the parent and only 7% of that of the 2 hour sample. The conventional Guinier plots of log $I(Q)$ against Q are shown as an insert to figure 4. They all exhibit strong curvature which indicate that particles with a range of sizes are present. The graph for the parent sample is the distinct lower curve. All of these graphs are linear at the smallest Q values where a radius of gyration can be obtained having a value of 450 Å for the parent sample and 350 Å for the MA specimens. It can be concluded from this that there are some, as yet unidentified, features on this length scale present throughout the reaction.

4. Discussion

The neutron diffraction patterns of the parent, 2 and 4 hour samples are dominated by the Bragg peaks of the nickel and molybdenum, while that for the 8 hour sample is different

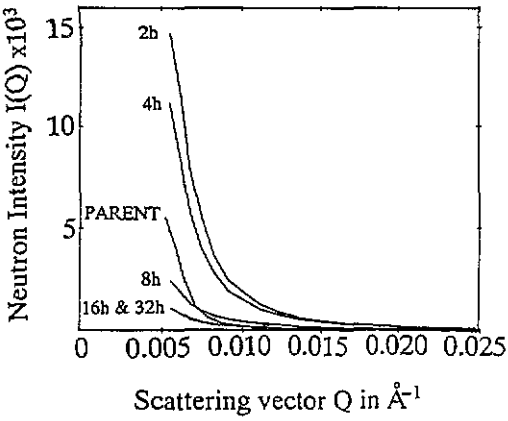

Figure 3. The intensity of the small angle scattering signal $I(Q)$ is plotted as a function of Q for the six $Ni_{50}Mo_{50}$ samples.

from those for the three shorter MA times. The patterns of the 16 and 32 hour samples show clearly that both consist of an amorphous phase and some free molybdenum. However this rather discontinuous picture of the amorphization process probably arises because these samples monitor the reaction at discrete times. The present study is not a real-time investigation of the reaction, as is possible with the multilayer amorphization reaction [23] or the hydrogen amorphization reaction [24]. Thus the fact that 8 hours of MA treatment almost coincides with the disappearance of the nickel in the sample is probably fortuitous and gives a misleading view of the continuity of the reaction.

In order to quantify the consumption of the nickel and molybdenum in the reaction, the intensities of the Bragg peaks were measured out to a Q value of 13 $Å^{-1}$ and the sums of these intensities $\sum I$ are given in table 1. Note that the ratio between the sums of the Bragg peak intensities of the nickel and the molybdenum in the parent sample, (4.428/2.267 = 1.95) in table 1, is in fair agreement with the ideal ratio $R = N_{Ni}b_{Ni}^2/N_{Mo}b_{Mo}^2$ which is $R = (b_{Ni}/b_{Mo})^2 = (1.03/0.695)^2 = 2.20$ for a parent alloy of equiatomic concentration. Despite the limited number of data points, the disappearance of the Bragg peaks for both nickel and molybdenum can be approximated by an equation of the form

$$\sum I = \sum I_0 \exp(-t/\tau)$$

with $\tau_{Ni} \simeq 4.4$ h and $\tau_{Mo} \simeq 5.9$ h. The former figure is in good agreement with the value $\tau_{Ni} \simeq 4.1$ h obtained by us from SQUID magnetometry measurements [21] and the latter commensurate with the characteristic time, $\tau_{Mo} \simeq 5.4$ h, for the *broadening* of the Bragg peaks in the x-ray diffraction patterns reported in that study. These sums of the Bragg peak intensities can, when normalized, be used to estimate the constitution of the samples during the reaction, as shown in the lower part of table 1. Clearly the rapid consumption of the nickel in the early stages of the reaction, as indicated by the reduction of the Bragg peaks for the 0, 2 and 4 hour samples, must lead to other changes in those specimens, which can be estimated just from the conservation of the numbers of the atoms present. Table 1 shows that, if this material transforms directly to the amorphous phase, the 2 and 4 hour samples will have only 11% and 15% amorphous material present respectively. This is probably close to the limit of detection in the diffraction patterns, bearing in mind the inherently low visibility of the diffuse scattering [25]. The amorphous phase is estimated to be about 66% of the 8 hour sample and this is consistent with the changes observed between the diffraction patterns of both the 2 and 4 hour samples and the 8 hour one.

A further insight into the nature of the changes taking place in the specimens is given by the SAS data particularly when they are plotted as log $I(Q)$ versus log Q, see figure 4. The

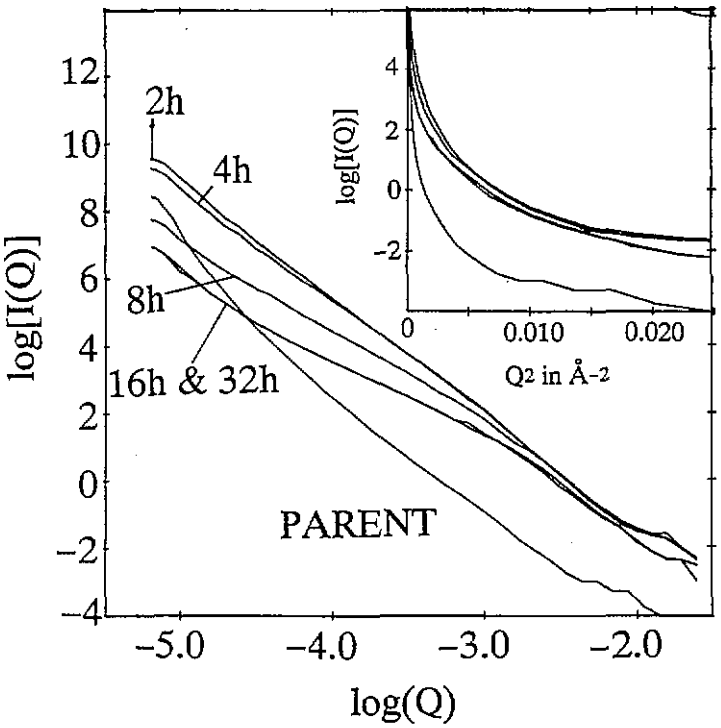

Figure 4. The neutron small angle intensity data are presented as log $I(Q)$ against log Q for the six $Ni_{50}Mo_{50}$ samples. The inset shows the corresponding Guinier plots, log $I(Q)$ versus Q^2 whose curvature indicates that there is a range of crystallite sizes present in the samples.

use of such graphs has become widespread, stimulated by studies of systems which exhibit fractal characteristics. The slope of the graph S can be related to the fractal dimension D of the interfaces between different regions of the sample, according to the relation $S = 6\text{-}D$ [26]. In figure 4 the graph for the parent is curved, even on this log–log scale, but the graphs for the 2 and 4 hour samples are linear over a wide Q range. The graphs for the 16 and 32 hour samples are also similar to one another and appear to show two regions of slope similar to the 2 and 4 hour samples. The graph for the 8 hour sample appears to be intermediate between those of the 2 and 4 hour and the 16 and 32 hour specimens. These data were derived from a very preliminary experiment and, as yet, it has not been possible to address the question of surface scattering by the contrast matching technique. However there is some evidence from more recent trials by us on NiTi specimens [27] and independent SAS measurements [28] on CuTi specimens made by the MA method, that the observed scattering is not due to surface effects. In addition, the similarities between the sequence of changes observed in these SAS data and the sequence of changes observed in the diffraction patterns of figure 2 provide some evidence that the changes seen are not surface effects. The slope of the SAS graphs of the 2 and 4 hour samples in figure 4 is −3.4 so this is consistent with rough surfaces between different regions of those samples which have a fractal dimension of 2.6. Whilst the origin of these effects is not known, we can postulate that the surfaces are those between the nickel and molybdenum particles of the sample. Optical micrographs of powder particles fused together after short milling times show very convoluted profiles of the constituents, see for example figure 1, of Hellstern and Schulz [29]. It is probably unwise to attempt an interpretation of the log–log graphs of

the other specimens which are linear over more restricted ranges in log Q.

The peak intensity values in table 1 show that the fraction of molybdenum left unconsumed in the reaction appears to be tending towards 40%, i.e. $\simeq 1.063/2.267 \simeq 0.984/2.267 \simeq 0.40$. The final composition of the amorphous NiMo phase may therefore be close to $Ni_{50}Mo_{50\times0.6} = Ni_{62}Mo_{38}$, and this is almost identical with the estimate of '$Ni_{50}Mo_{31}$' obtained by us earlier [17,18]. It is not possible, incidentally, to remove the excess molybdenum by just increasing the concentration of nickel in the starting material. Trudeau and Schultz [30] have, in fact, examined nickel-rich NiMo alloys, but they have found only nano-crystalline structures. On the basis of having detected very high levels of iron contamination [15–20 atomic percent] in *their* NiMo samples milled in steel vials, they have suggested that the samples produced *by us* previously, must have been aided and stabilized by iron contamination. Quite apart from the fact that such high levels of contamination of a crystalline phase would be visible in x-ray diffraction, our recent SQUID magnetometry measurements, which are very sensitive [21], have shown quite clearly that no such gross contamination occurs. A $Ni_{50}Mo_{50}$ sample ball milled by us in a steel vial under argon for 48 hours, for example, had a small residual magnetization consistent with there being 2.3% of the original nickel still unreacted. If this magnetization arose instead from an iron impurity, the fraction present would reduce below 0.7% because the iron has a larger magnetization. This value is not compatible with the much higher figures quoted by Trudeau and Schultz [30].

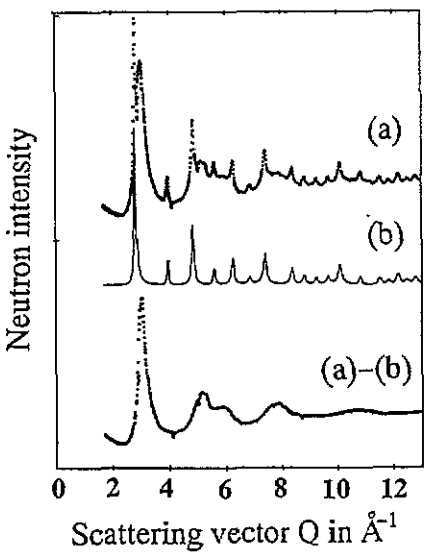

Figure 5. The procedure used to separate the crystalline and amorphous components of the neutron diffraction pattern of the $Ni_{50}Mo_{50}$ specimen (a) MA treated for 32 hours, is shown. The pattern of crystalline molybdenum (b) is recovered numerically after profile fitting and then subtracted from the experimental curve as shown.

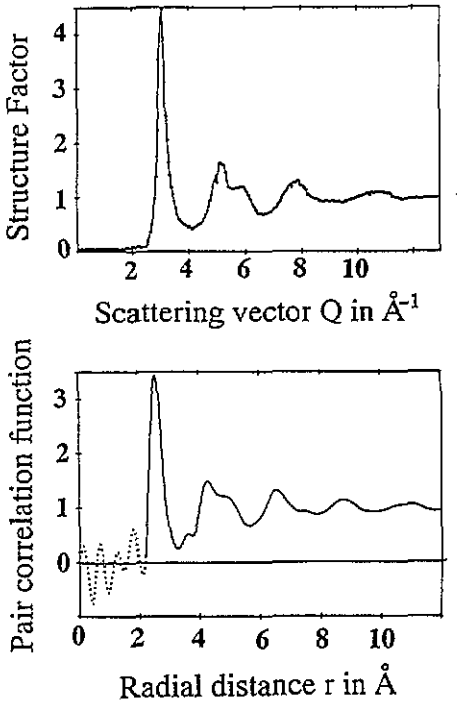

Figure 6. The total structure factor $S(Q)$ of the $Ni_{50}Mo_{50}$ specimen MA treated for 32 hours, which was derived from the diffraction pattern given in figure 5, is shown in the upper figure. The pair correlation function $g(r) = \rho(r)/\rho_0(r)$ derived from it by Fourier transform is given in the lower figure.

In addition to information about the timescales of the reaction, we were interested in determining the structure of the transformed amorphous NiMo alloy and have used the peak fitting program developed by us earlier [31] to subtract the Bragg peaks of the crystalline molybdenum. The peak shape for pulsed neutron scattering is a complex asymmetrical function involving two exponentials [19] but when broadened, as in the present case, a skewed curve of the type used by us previously [31] seems to result in an acceptable fit. Figure 5(a) gives the neutron diffraction pattern of the 32 hour sample and figure 5(b) the synthesized pattern of the BCC molybdenum which was produced. The lower figure shows this subtracted from the original, in order to give the diffuse pattern of the amorphous phase. This latter pattern was then normalized by the $I(0)$, $I(\infty)$ method [32], to give the total structure factor shown in figure 6. This curve was Fourier transformed to give the pair correlation function shown in the lower part of figure 6. This $g(r)$ has a similar form, in the positions and relative magnitudes of the peaks, to the $g(r)$ function of an amorphous $Ni_{50}Mo_{50}$ specimen prepared by sputter deposition [33]. The present first-neighbour distance of 2.54 Å is slightly lower than the value from the sputtered sample [33]. This is not unexpected since the present NiMo specimen is not precisely equiatomic as discussed above. In addition, the large neutron scattering amplitude of nickel will emphasize the weighting factor for the Ni–Ni correlations in the $g(r)$ curve. The first-neighbour distance of 2.54 Å agrees with the value of 2.56 Å estimated by applying the Ehrenfest relation to the position of the first amorphous halo in the x-ray diffraction patterns of the NiMo alloys studied by us previously [17, 18]. The overall similarity between the pair correlation functions of the present sample and the amorphous $Ni_{50}Mo_{50}$ sputtered sample together with the 'conventional' appearance of the total structure factor is most encouraging. They illustrate that genuine amorphous alloys can be produced even in those reactions which are 'incomplete' in the sense of having some fraction of the starting material unconsumed.

5. Conclusions

The amorphization reaction in $Ni_{50}Mo_{50}$ alloys has been studied by neutron diffraction and neutron small angle scattering and it has been confirmed that 32 hours of MA treatment leads to the production of a two-phase sample having an amorphous component with a composition close to $Ni_{62}Mo_{38}$ and some free molybdenum. The strong scattering from the nickel, which occurs with neutrons, has allowed some estimates to be made of the timescales of the reaction. The sequence of the changes observed in the diffraction experiments agrees well with that seen in the small-angle scattering experiments. The small-angle scattering data for the 2 and 4 hour samples provide evidence for the existence of rough surfaces having fractal characteristics between different parts of those samples. We tentatively associate this with the type of convoluted interfaces observed between the alloy constituents in optical micrographs. A characteristic of fractals is the repetition of a motif by simultaneous translation, rotation and reduction (as opposed to just translation in crystallography). It is not surprising therefore, that fractal characteristics should be seen in alloy composites in the early stages of the MA process by ball-milling. The reduction in size of the constituents and the welding together and folding and bending of the particles to produce a filamentary composite was, in fact, fully described by Benjamin in his seminal articles in the 1970s [34, 35].

We propose to extend these measurements to alloys having shorter periods of MA treatment in order to obtain a more accurate measurement of the consumption of the constituents. In addition, further neutron small-angle scattering experiments are in hand, in

which the contrast matching technique will be used in order to isolate the scattering from the surfaces of the powder particles.

Acknowledgments

This work has been supported by ENEA contract 3965 and CNR contract 89.00605.69. The collaboration between Dr Cowlam and Professor Cocco is supported by a Royal Society/CNR Travel Grant. The neutron measurements were made at ISIS, Rutherford Appleton Laboratory, Chilton under the aegis of the neutron beam programme of the SERC and the help of Dr Howells and Dr Heenan are gratefully acknowledged. Mr Li has been supported through the Technical Cooperation Training Programme of the Sino–British Friendship Scholarship Scheme.

References

[1] Schwarz R B and Johnson W L (ed) 1988 *Conf. on Solid State Amorphising Transformations* (Los Alamos National Laboratory, 1987) *J. Less-Common Met.* 140
[2] Weeber A W and Bakker H 1988 *Physica* B **156** 93–135
[3] Cargill G S 1975 *Solid State Phys.* **30** 227–329
[4] Ivison P K, Soletta I, Cowlam N, Cocco G, Enzo S and Battezzati L 1992 *J. Phys.: Condens. Matter* **4** 1635–45
[5] Ivison P K, Cowlam N, Soletta I, Cocco G, Enzo S and Battezzati L 1991 *Mater. Sci. Eng.* A **134** 859–62
[6] Koch C C, Cavin O B, McKamey C G and Scarbrough J O 1983 *Appl. Phys. Lett.* **43** 1017–20
[7] Guinier A 1963 *X-ray Diffraction* (San Francisco: Freeman)
[8] Cocco G, Enzo S, Schiffini L and Battezzati L 1988 *Mater. Sci. Eng.* **97** 43–6
[9] Ohering M and Bormann R 1991 *Mater. Sci. Eng.* A **134** 1330–3
[10] Wagner C N J and Boldrick M S 1991 *Mater. Sci. Eng.* A **133** 26–32
[11] Warren B E and Averbach B J 1950 *J. Appl. Phys.* **21** 595–9
[12] Williamson G K and Hall W H 1953 *Acta Metall.* **1** 1–22
[13] Cocco G, Soletta I, Enzo S, Magini M and Cowlam N 1990 *J. Physique* C4 181–7
[14] Windsor C G 1981 *Pulsed Neutron Scattering* (London: Taylor and Francis)
[15] Howells W S 1980 *Rutherford Appleton Laboratory Report* RL-80-017
[16] Heenan R K, Osborn R, Stanley H B, King S M, Mildner D F R and Furusaka M *J. Appl. Crystallogr.* to be submitted
[17] Cocco G, Enzo S, Barrett N and Roberts K J 1989 *J. Less-Common Met.* **154** 177–86
[18] Cocco G, Enzo S, Barrett N and Roberts K J 1992 *Phys. Rev.* B **45** 7066–76
[19] Soper A K, Howells W S and Hannon A C 1989 *Rutherford Appleton Laboratory Report* RAL-89-046
[20] Li M unpublished
[21] Cowlam N, Crangle J and Li M *J. Magn. Magn. Mater.* submitted
[22] Heenan R K 1989 *Rutherford Appleton Laboratory Report* RAL-89-129
[23] Zarbakhsh A, Cowlam N, Highmore R J, Evetts J E, Penfold J and Shackleton C 1990 *J. Phys.: Condens. Matter* **2** 2537–45
[24] Cowlam N, Titman J M and Wright M S 1989 *Z. Phys. Chem.* **163** 325–30
[25] Hunt J, Soletta I, Battezzati L, Cowlam N and Cocco G *J. Alloys Compounds* at press
[26] Bale H D and Schmidt P W 1984 *Phys. Rev. Lett.* **53** 596–9
[27] Cowlam N, Cocco G, Enzo S and Battezzati L 1991 *ISIS Exp Report* RB/3068
[28] Hannon A C and Atzmon M 1989 *ISIS Exp Report* RB/2589
[29] Hellstern E and Schulz L 1986 *Appl. Phys. Lett.* **48** 124–6
[30] Trudeau M L and Schultz R 1991 *Mater. Sci. Eng.* A **134** 1361–7
[31] Enzo S, Benedetti A and Polizzi S 1985 *Z. Kristall.* **170** 275–83
[32] Enderby J E 1968 *Physics of Simple Liquids* ed H N V Temperley, J S Rowlinson and G S Rushbrooke (Amsterdam: North-Holland)
[33] Aur S, Kofalt D, Waseda Y, Egami T, Wang R, Chen H S and Boon-Keng Teo 1883 *Solid State Commun.* **48** 111–5
[34] Benjamin J S 1976 *Sci. Am.* **234** 40–8
[35] Benjamin J S and Volin T E 1974 *Metall. Trans.* **5** 1929–35